# Evidence for massive Black Holes in the Nuclei of Active Galaxies from Gamma-Ray Observations

Werner Collmar, and Volker Schönfelder

Max-Planck-Institut für extraterrestrische Physik, Postfach 16 03, D-85740 Garching, Germany

**Abstract.** According to our present knowledge Active Galactic Nuclei (AGN) consist of a massive black hole, which accretes matter from its environment. By this process the gravitational energy is converted into electromagnetic radiation. Before the launch of the Compton Gamma-ray Observatory (CGRO) only four AGN had been reported to emit detectable gamma-rays. Now, after roughly six years in orbit, the different CGRO experiments have discovered about 90 AGN in the energy range between 50 keV and 20 GeV. So, CGRO finally opened the field of extragalactic gamma-ray astronomy. Two main conclusions can be drawn from the CGRO-results: 1) Seyfert galaxies are hard X-ray sources rather than gamma-ray sources. They emit thermal radiation which cuts off at energies above a few hundreds of keV (~200 keV). 2) Radio-loud quasars and BL Lac-objects - so called blazars - however, can be strong gamma-ray emitters up to energies of at least several GeV. They show a highly variable non-thermal emission component. The assumption of isotropic emission together with the observed variability would lead to a high radiation density in a small emission region. At least for some sources the derived compactness is in conflict with the assumption of isotropy and therefore relativistic beaming of the gamma emission is strongly suggested. The observed broad band $\nu F_\nu$-spectra show a maximum at gamma-rays. However, taking into account the relativistic beaming the gamma-ray energy output is a factor of up to $10^4$ smaller than suggested by the observed intensity spectra.

We discuss these CGRO results in the context of the gamma-ray emission processes, AGN emission models, and conclude on the evidence for massive black holes in the center of active galaxies.

## 1 What are 'active' Galaxies in Comparison to 'normal' Galaxies

The observable universe consists of billions of galaxies, many of them containing 100 billion or more stars, like our 'Milky Way' for example. On a morphological basis these galaxies are grouped into three main categories: spirals, ellipiticals, and irregulars.

In 1943 the US astronomer Carl Seyfert noted a distinct class of galaxies with stellar appearing cores and broad nuclear emission lines. Galaxies, showing these two characteristica, were subsequently named 'Seyfert' galaxies and mark today a sub-class of the so-called 'Active Galaxies'. Active galaxies comprise names like 'quasars' (quasi-stellar radio sources), 'QSOs' (quasi-stellar objects), 'Markarian galaxies', 'radio galaxies', and 'blazars' for example. The names of

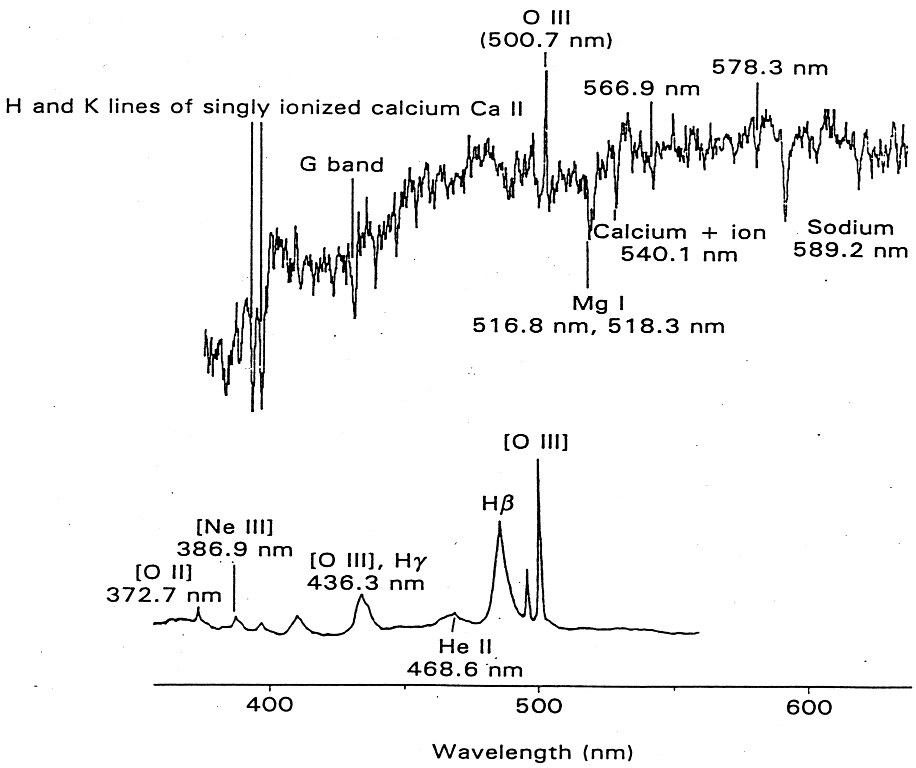


Fig. 1: Comparison of optical spectra from a 'normal' (spiral) galaxy above and an 'active' (Seyfert) galaxy below. The spectrum of the spiral galaxy shows mainly absorption lines due to stars, while the spectrum of the Seyfert galaxy is dominated by strong and broad emission lines. This figure is from Robson (1997).

the different sub-classes of active Galaxies developed historically according to the name of the reporting astronomer (e.g. 'Seyferts', 'Markarians'), morphological characteristica (QSOs), or from other properties.

There are distinct observational differences between ordinary or 'normal' galaxies and 'active' galaxies. In contrast to the images of 'normal' galaxies, which are basically an assembly of stars, the images of active galaxies show bright nuclei. Their optical spectra typically show broadened emission lines instead of absorptions lines (Fig. 1). Their overall spectra show luminosity maxima in IR, UV, X- or even $\gamma$-rays, and are often dominiated by non-thermal emission, while normal galaxies radiate most of their energy in the optical band simply being the sum of the starlight. Another major difference between 'normal' and 'active' galaxies is the variability. While normal galaxies always look the same -

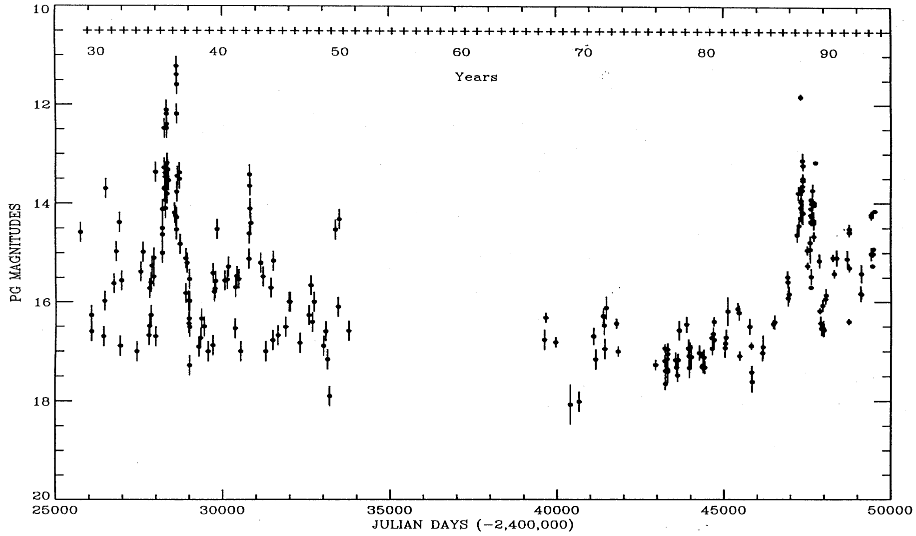


Fig. 2: Time history of the quasar 3C 279 in the optical band from 1930 to 1994. Variations up to ∼7 magnitudines (a factor of ∼630) are observed. The 'activity' of the source is obvious. The figure is from Hartman et al. (1996).

may be a supernova is brightening occasionally for a few month - the emission of active galaxies changes significantly on short time scales (Fig. 2) down to days or even below, which - in our mind - gave rise to the term 'active'. This short-term variability points to small sizes of the emission regions which are consistent with the bright nuclei. In the specific case of quasars or QSOs the nucleus overshines the rest of the galaxy by far resulting in a starlike image. On the basis of light-travel arguments, the emission region radius is estimated to

$$r < c\Delta t/(1+z) \ , \tag{1}$$

with $\Delta$t the observed time variability, z the redshift of the source, and c the speed of light. Some active galaxies show jets like the famous quasar 3C 273 for example.

## 2 A Unification Scheme for AGN

Roughly 3% of all galaxies are classified as being 'active'. Although there is no overall agreement amongst astronomers about a precise definition of active galaxies, one common criterium is the generation of large luminosties in small core regions. In many cases the active and bright core overshines the remaining galaxy by far.

As described above there exist a large number of classes and sub-classes, which developed historically and sometimes overlap in their parameters, and which are confusing physicists and even astrophysicists not working in AGN research. For example the most luminous Seyferts are brighter than the low-luminous quasars. If such a Seyfert galaxy would be 'put' far out to cosmological distances, only the bright core remains visible, and, subsequently, it would be classified as a QSO ('quasi-stellar object'). So, in a first step of unification, it is suggested that some Seyferts are simply 'nearby quasars'.

Table 1: This table (from Urry and Padovani 1995) shows the simplified classification of AGN according to the two parameters 'radio-loudness' and 'optical emission line properties'. The main types of AGN are sorted into the table. The abbreviations have the following meaning: NLRG, BLRG: narrow, broad line radio galaxies, SSRQ, FSRQ: steep, flat spectrum radio quasars, FR I, II: Fanaroff-Riley Type 1,2 radio galaxies, and BL Lac: BL Lacertae object. For a more detailed description of the different types see e.g. Urry and Padovani (1995) or Robson (1997).

| Radio Loudness | Optical Emission Line properties | | | |
|---|---|---|---|---|
| | Type 2 (Narrow Line) | Type 1 (Broad Line) | Type 0 (unusual) | |
| radio-quiet (85-90%) | Seyfert-2 | Seyfert-1 QSO | | ? ↑ |
| radio-loud (10-15%) | NLRG (FR I, FR II) | BLRG SSRQ, FSRQ | Blazars (BL Lac, FSRQ) | ↓ ? |
| | decreasing jet angle to line of sight → | | | |

Observationally, AGN are classified on the basis of three parameters: the strength of their radio emission, the emission line properties in the optical and UV range, and the luminosity. However, the question was asked, whether there is some common underlying physics or physical structure involved. One of the first steps towards unification concerned the difference between the two sub-classes of Seyfert galaxies simply called 'Type 1' and 'Type 2'. While the 'Type 1' Seyferts show broad - ($\Delta v > 2000$ km/s) and narrow emission lines ($\Delta v < 2000$ km/s), the 'Type 2' sources show only narrow emission lines. A key observation by Antonucci and Miller (1985) revealed weak broad lines in polarized light from the Seyfert-2 galaxy NGC 1068. Since scattered light is polarized, this observation was interpreted that NGC 1068 also generates broad emission lines, which however, are somehow hidden from direct observation. From such observational facts a simplified classification scheme evolved recently which is shown in Table 1 (Urry and Padovani 1995). The different classes of AGN are ordered according to two parameters only: their 'optical emission line properties' and their 'radio loudness'.

With respect to their line properties, AGN are subdivided into so called 'Type-2' sources showing only narrow emission lines, 'Type-1' sources showing also broad emission lines, and 'Type-0' sources showing an unusual behaviour, e.g. weak or even absence of any lines. AGN are considered to be radio-loud if the ratio of the radio flux at 5 GHz to the optical B-band ('blue') flux is larger than 10 ($f_{5GHz}/f_B \geq 10$) (Kellermann et al. 1989). According to this definition roughly 10% to 15% of all AGN are radio-loud.

The different main AGN types are sorted into this two-dimensional scheme accordingly (Table 1). It is believed that the horizontal axis reflects an orientation effect, namely the decreasing angle to the line of sight towards the jet of an active galaxy (see Fig. 3). There is no commonly accepted interpretation why some AGN are radio-loud and others not. Whether this has to do with the host galaxy - radio-loud sources are mainly found in elliptical galaxies, while radio-quiet ones in spirals - or with the spin of the putative central BH or something else remains unclear to date. This question is currently one of the major unresolved problems in AGN research.

Fig. 3 shows the 'standard model' for AGN, which explains the different types as simply being an orientational effect. Despite the fact that many details are not yet understood, the scenario - which is described in the following - is commonly accepted because it explains the major observational facts reasonably well and consistently. The central object is thought to be a supermassive Black Hole (BH) with masses of the order of $\sim 10^6$ to $\sim 10^{10}\,M_\odot$. The Schwarzschild radius ($R_s = 2GM_{BH}/c^2$) of an $10^8\,M_\odot$ BH is $\sim 3 \cdot 10^8$ km, which is approximately 2 Astronomical Units (AU) or $\sim 10^{-5}$ parsecs (pc). The BH is surrounded by an accretion disc consisting of ionized material reaching out to several hundreds of Schwarzschild radii. This very center of an active galaxy is surrounded by an extended molecular torus with an inner diameter of $\sim$1.5 pc and an outer diameter of the order of $\sim$30 pc. Within the molecular torus and near the center of the active galaxy fast moving (v$\geq$2000 km/s) gas clouds (dark spots in Fig. 3) exist which are ionized by the accretion disk radiation and which emit the observed broad emission lines. These fast moving clouds are located within $\sim 2\text{-}20 \cdot 10^{16}$ cm and are marking the so called 'broad-line region' (BLR). Further out such clouds (grey spots in Fig. 3) move slower (v$\leq$2000 km/s) and therefore give rise to the observed narrow emission lines. This so-called narrow-line region (NLR) ranges roughly from $10^{18}$ cm to $10^{20}$ cm. In addition to these clouds a hot electron corona (dark dots in Fig. 3) populates the inner region which can scatter some continuum and broad line emission as was observed in NGC 1068 (Antonucci and Miller 1985). In a radio-loud AGN a strong jet of relativistic leptons emanates perpendicular to the plane of the accretion disc. The generation of such jets is still not understood, however it is believed that strong magnetic

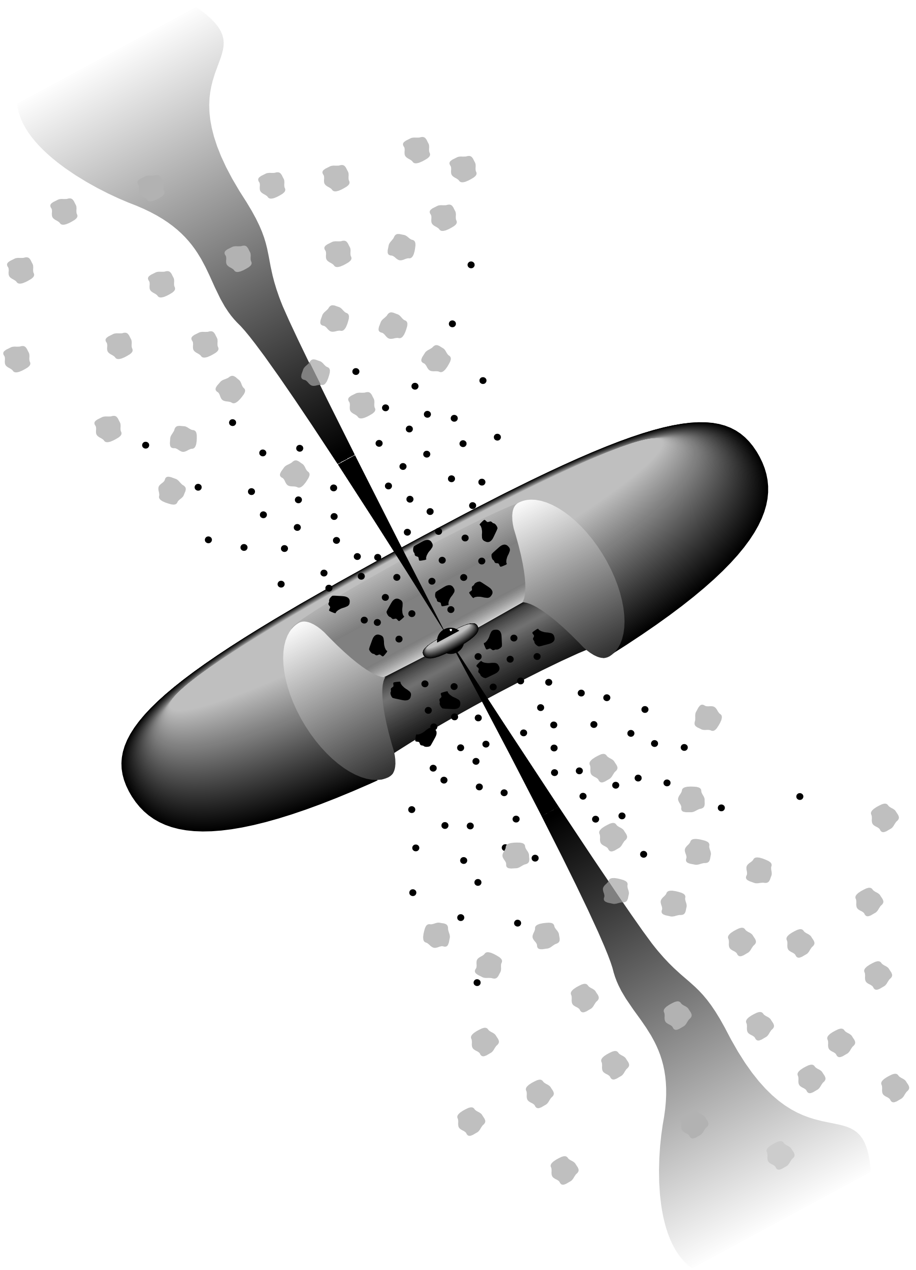

Fig. 3: The 'standard model' for radio-loud AGN. For an explanation see the text. The plot is from Urry and Padovani (1995).

fields play a fundamental role. Radio jets have been observed on scales from $10^{17}$ cm to $\sim 10^{24}$ cm, which is significantly larger than the largest galaxies.

The 'unification-by-orientation' scenario assumes such a general structure for all AGN. Depending on the spatial orientation with respect to us we observe the different types of AGN. If we look towards the 'central engine' along the jet axis ($<10^o$) i.e. basically directly into the jet, we observe a blazar. A regular quasar or a Seyfert-1 galaxy is observed if we look at an offset angle of the order of $30^o$, at which both the narrow- and broad-line region are visible. At larger angular offsets the broad-line region will be hidden by this extended molecular torus giving rise to Seyfert-2 galaxies. A typical radio galaxy, showing two strong opposite jets, is observed at angles approximately perpendicular to the jet axis.

This scenario is very intriguing and is widely accepted among astronomers. However, there are still several unresolved questions like 'Where are the radio-quiet and narrow-line (Type 2) QSOs?', and 'What causes the difference between radio-loud and radio-quiet AGN?'. In addition, this scenario neglects evolution, which probably is another important parameter for active galaxies.

## 3 Gamma-ray Emission of AGN

The $\gamma$-ray domain of the electromagnetic spectrum is located at photon energies above $\sim$500 keV, still containing the 511 keV electron-positron annihilation line. Due to absorption in the earth atmosphere, $\gamma$-ray observations in the MeV - to GeV-range have to be carried out from space. Currently this is mainly done by the Compton Gamma-Ray Observatory (CGRO), which was launched on April 5, 1991 (Fig. 4). CGRO is a NASA satellite, with contributional experiments from Europe, mainly Germany. CGRO carries four different experiments, which in total cover an energy range from 20 keV to $\sim$30 GeV and which are supplementary in energy range. Their main characteristica are given in Table 2.

Table 2: The four scientific instruments aboard CGRO

| Instrument | Energy Range [MeV] | Field-of-View |
|---|---|---|
| OSSE (Oriented Scintillation Spectroscopy Exp.) | 0.05 - 10 | $3.8^o$x $11^o$ |
| COMPTEL (Compton Telescope) | 0.75 - 30 | $\sim$1 sr |
| EGRET (Energetic Gamma-Ray Telescope Exp.) | 20 - 30000 | $\sim$0.5 sr |
| BATSE (Burst and Transient Source Exp.) | 0.02 - 10 | all-sky |

Before CGRO only four AGN had been reported to emit detectable $\gamma$-rays. The radio galaxy Centaurus A (v. Ballmoos et al. 1987) and the Seyfert galaxies

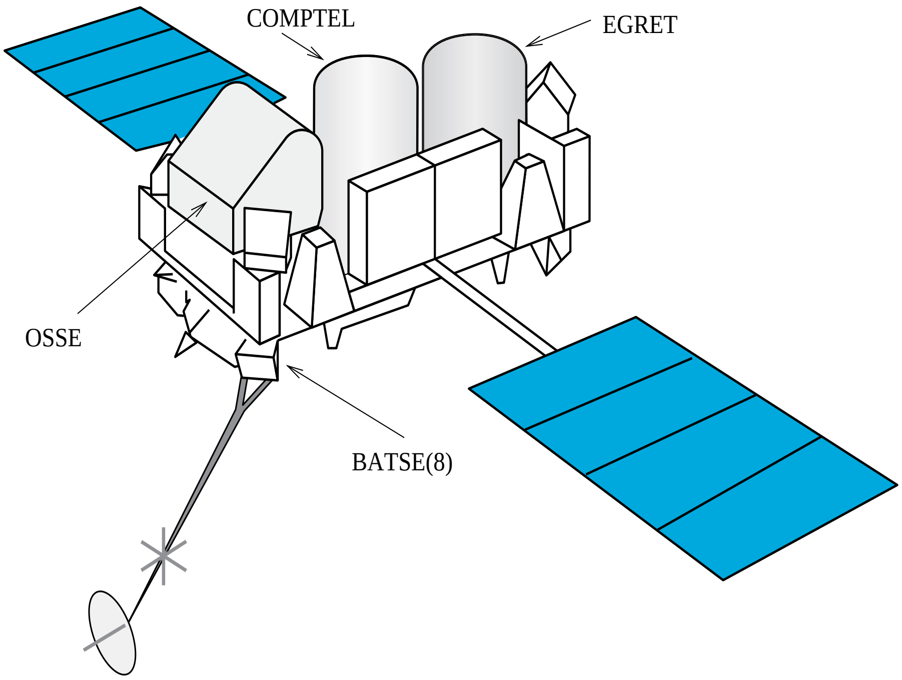


Fig. 4: Schematic view of the Compton Gamma-ray Observatory. The four different experiments are indicated. BATSE, in contrast to the others, is designed to be an all-sky monitor with the prime goal to observe $\gamma$-ray bursts. Therefore it consists of 8 detectors, which are located at the edges of the spacecraft and are pointing to different directions.

NGC 4151 and MCG-8-11-11 (Perotti et al. 1981a, 1981b) up to energies of $\sim$20 MeV. The quasar 3C 273 was the fourth one, which was only detected at the high-energy end above 50 MeV by the Cos-B satellite (Swanenburg et al. 1978). In view of the improved sensitivities of the CGRO instruments with respect to previous experiments, it was expected prior to the launch that CGRO would detect several quasars, Seyfert -, and radio galaxies. In addition, there was the hope for new und and unexpected discoveries which is usually the case when improved instruments come into operation.

### 3.1 Blazars

Because 3C 273 was a prime candidate for $\gamma$-ray emission, CGRO was pointed shortly after launch towards this quasar. Indeed, a strong $\gamma$-ray signal was im-

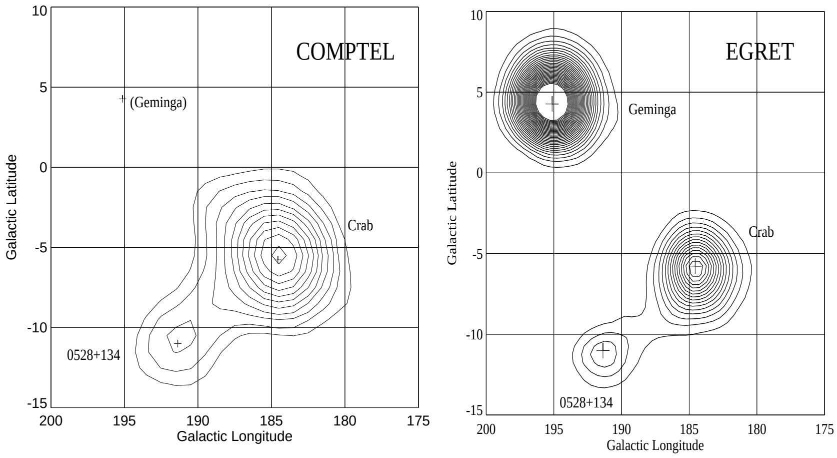


Fig. 5: Comparison of COMPTEL (10-30 MeV) and EGRET (>100 MeV) significance maps at the galactic anticenter. Three significant sources are seen by EGRET: the previously known galactic pulsars Crab and Geminga, and the newly discovered $\gamma$-ray blazar PKS 0528+134. The absence of Geminga in the COMPTEL maps is due to its hard spectrum, which causes it to fall below the COMPTEL detection threshold despite its prominence in the EGRET data. This figure is from Hartman et al. (1997).

mediately observed by the EGRET experiment. However, this signal was not at the 'right' location. It was offset by $\sim 8^o$ from the position of 3C 273, thereby causing some confusion within the EGRET and satellite operations teams. After the satellite pointing and the EGRET data analysis was confirmed to be correct, the strong $\gamma$-ray source was identified with the blazar-type quasar 3C 279. 3C 279, known to be a radio source and an optically violently variable quasar, was the most 'dramatic' object inside the EGRET location error box. Further observations of other sky regions often showed a fairly bright $\gamma$-ray source in the EGRET field-of-view and their error boxes always contained a blazar-type AGN, supporting the identification of 3C 279. So, after some time of operation, the conculsion that blazars can - at least occasionally - be strong emitters of $\gamma$-ray radiation became firm. Blazars are radio-loud quasars or BL Lac objects, which show a flat radio spectrum, strong and rapid variability in both optical and radio bands, and strong optical polarization. In addition, many blazars show superluminal motion of radio 'knots' resolved by very long baseline interferometry (VLBI).

After 5 years of operation, roughly 70 blazars have been detected by EGRET at energies above 100 MeV (Kanbach 1996). Eight of them are observed also at low-energy $\gamma$-rays by COMPTEL (Collmar 1996), and also eight by the OSSE experiment (McNaron-Brown et al. 1995) mainly at hard X-ray energies ($\sim$50 keV

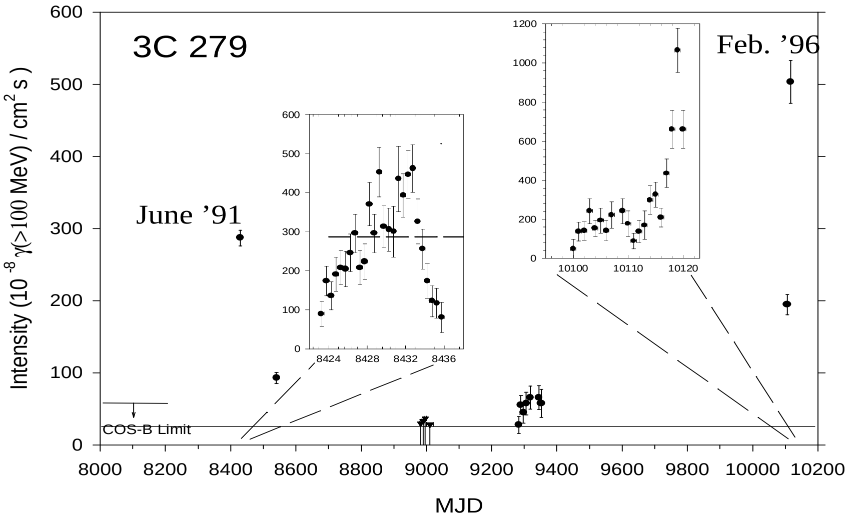


Fig. 6: Time history of fluxes, including flaring events, of 3C 279. For details see the text. The figure is from Hartman et al. (1997).

to ~500 keV). Figure 5 shows simultaneous COMPTEL and EGRET maps of the galactic anticenter region. The evidence for the newly discovered $\gamma$-ray blazar PKS 0528+134 is obvious in both maps.

The $\gamma$-ray fluxes are observed to be highly variable with variability time scales, e.g. doubling of the flux, of years down to less than one day. In some sources strong flux variations, up to a factor of 80, have been observed. A prominent example, the long-term $\gamma$-ray light curve of 3C 279 as observed by EGRET at energies above 100 MeV is shown in Figure 6. Short-term varaibility (~days) is clearly seen in the insets, which resolve the two major $\gamma$-ray flares observed from this blazar.

The energy spectra measured by the different CGRO instruments are consistent with power-law shapes. However, if they are combined a spectral turnover at MeV-energies becomes evident (Fig. 7) for several blazars. This indicates that the MeV-range is a spectral transition region for blazars (see also Figs. 8, 9). Integrating the observed spectra and assuming isotropic emission of the distant sources results in source luminosities of $\sim 10^{48}$ erg/s on average with a maximum of $\sim 5 \cdot 10^{49}$ erg/s for the $\gamma$-ray band above 1 MeV.

### 3.2 Seyfert - and Radio Galaxies

Seyfert galaxies, Type 1 as well as Type 2, have not fulfilled the expectations about prominent $\gamma$-ray emission. It was found by the OSSE experiment (e.g.

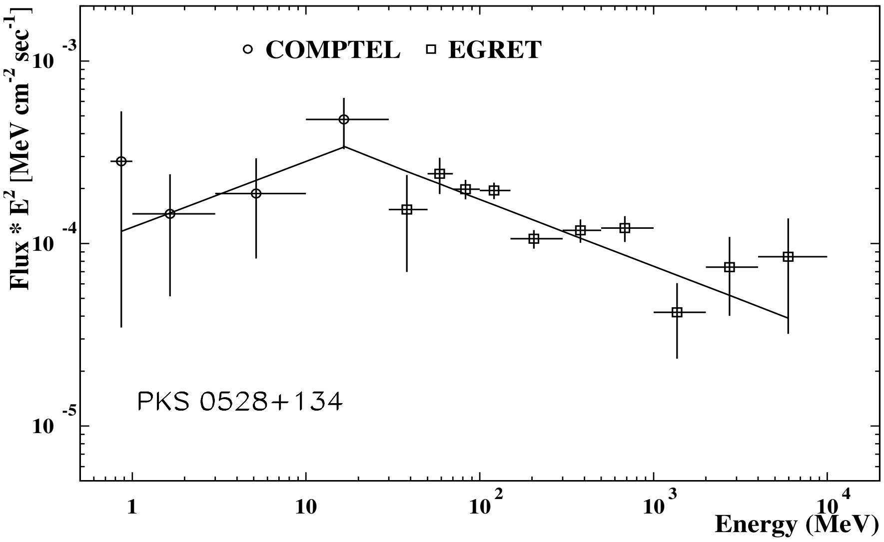


Fig. 7: Simultaneous EGRET and COMPTEL spectrum of the blazar PKS 0528+134 for a $\gamma$-ray flare. The solid line represents the best-fitting 'broken' power-law function. The spectral turnover at MeV-energies is evident. The figure is from Collmar et al. (1997).

Johnson et al. 1997) that the spectra of Seyfert galaxies cut off at energies around $\sim$100 to $\sim$200 keV showing the signature of a thermal spectrum (see Fig. 10). No Seyfert galaxy has yet been detected by COMPTEL and EGRET.

Cen A, the closest active galaxy ($\sim$4 Mpc), is the only radio galaxy detected so far at hard X-rays and $\gamma$-rays. Cen A is a peculiar object with a Seyfert-2 type nucleus with strong optical extinction. Cen A was redetected by COMPTEL (Steinle et al. 1998) and probably also by EGRET (Nolan et al. 1996). However, source confusion is not completely ruled out in the case of the EGRET detection. Apart from Cen A no other radio galaxy has yet been detected by the CGRO experiments.

Because Seyferts are not $\gamma$-ray emitters and Cen A is a single and peculiar case we shall concentrate on the blazars for the rest of the paper.

## 4 Broad-band Properties of AGN

### 4.1 Gamma-Ray Production Processes

For the generation of $\gamma$-ray photons mainly non-thermal processes are responsible. Non-thermal means that the primary particles have a non-Maxwellian energy distribution, which is usually considered to be a power-law shape. Thermal emission is only of minor importance for the $\gamma$-ray emission, because in astrophysical environments the necessary plasma temperatures are only reached in exceptional cases. There are several processes to generate $\gamma$-ray photons (e.g. Schönfelder 1995). Here we shall concentrate on the ones important for the $\gamma$-ray blazars.

Sychrotron radiation is emitted when relativistic electrons interact with a magnetic field. The moving electrons are accelerated by the Lorentz force and radiate. The frequency of the synchrotron radiation $\nu_s$,

$$\nu_s \propto B \cdot E_e^2, \tag{2}$$

is proportional to the magnetic field strength B, and the square of the electron energy $E_e$. For example, $10^{13}$ eV electrons moving in a magnetic field of $10^{-4}$T would generate $\gamma$-ray synchrotron photons of $\sim$1 MeV. An electron cloud with a power-law distribution in energy will generate a power-law synchrotron spectrum. For a particle number spectrum of the form $N(E) \propto E^{-s}$ and a synchrotron photon number spectrum $N(E) \propto E^{-\alpha}$ the simple relation $\alpha=(s+1)/2$ between the two power-law indices holds.

The inverse Compton process describes the interaction between a low-energy photon and a high-energy electron. In this scattering process energy from the electron to the photon is transferred and the photons are scattered to higher energies according to the equation

$$\nu_{IC} \approx E_e^2 \cdot \nu_0, \tag{3}$$

where $\nu_{IC}$ is the frequency of the inverse Compton photon, $\nu_0$ the frequency of the soft photon, and $E_e$ the energy of the electron. For example, a MeV $\gamma$-ray is generated by the interaction of a UV-photon ($\sim10^{15}$ Hz) with a 0.5 GeV electron. Like in the synchrotron process also in the IC-process a power-law shaped electron distribution in energy generates a power-law shaped IC-spectrum with the same simple relation between the spectral indices.

The pair-production process is important in regions of high photon densities. This process describes the interaction of a high-energy $\gamma$-ray with another photon or the field of an atomic nucleus. Schematically this can be written as

$$\gamma + \gamma \rightarrow e^- + e^+, \quad \gamma + nucleus \rightarrow e^- + e^+ \ . \tag{4}$$

Because of simultaneous energy and momentum conservation this conversion can not occur for a single $\gamma$-ray photon. In the case of photon-photon interaction the following condition is valid

$$E_1 \cdot E_2 \geq \frac{2(m_e c^2)^2}{(1 - cos\alpha)}, \tag{5}$$

with $E_{1,2}$ the photon energies, $m_e$ the electron rest mass, c the speed of light, and $\alpha$ the interation angle between the photons. The inverse process

$$e^- + e^+ \rightarrow \gamma + \gamma \tag{6}$$

is also possible. The 511-keV annihilation line has been observed from the inner galaxy proving the pair-production process (generation of positrons) occurs in real astrophysical environments.

### 4.2 Multifrequency Observations of Gamma-Blazars

The CGRO observations of $\gamma$-ray blazars have shown that these sources can be enormously luminous at $\gamma$-ray energies and at the same time show short-term variability. Simultaneous multiwavelength spectra, and especially, multiwavelength monitoring have the potential of significantly increasing our knowledge about the physics of these spectacular sources. In simultaneous spectra from radio - to $\gamma$-ray energies the luminosity of the objects in different bands can be directly compared providing the possibility to identify the major emission components and - processes. Especially valuable would be the multifrequency monitoring because clues about correlated/uncorrelated time variability of different frequency bands are provided thereby revealing informations about their connections and possibly about their emission sites. For example, the information whether a X-ray - or optical flare occurs simultaneously, earlier, later, or is even absent during a $\gamma$-ray flare would be very constraining for the blazar modelling. To proceed in this direction several multifrequency campaigns have been organized around CGRO blazar observations. While the individual observations are easy to carry out, simultaneous observations of a particular source are difficult to achieve. Because telescope time is precious, especially on space experiments, severe pointing constraints exist, and scientific review panels have to be convinced, only a few examples of such campaigns were carried out with good coverage from the radio - to $\gamma$-ray band.

To date, probably the best result was derived for the blazar 3C 273, which is one of the best studied sources because it is the closest ($z = 0.158$) blazar-type quasar and is bright at all wavelength bands. Figure 8 (Lichti et al. 1995) shows a quasi-simultaneous multifrequency spectrum from radio - to TeV $\gamma$-rays of 3C 273. The ordinate represents the radiated power per natural logarithmic frequency interval, so the energy release in the different wavelength bands can directly be compared. First of all the spectrum shows that the high-energy emission (X- to $\gamma$-rays ) is a significant part of the bolometric luminosity. The spectrum shows (probably) four maxima indicating different emission components and processes, which are interpreted as synchrotron emission from relativistic

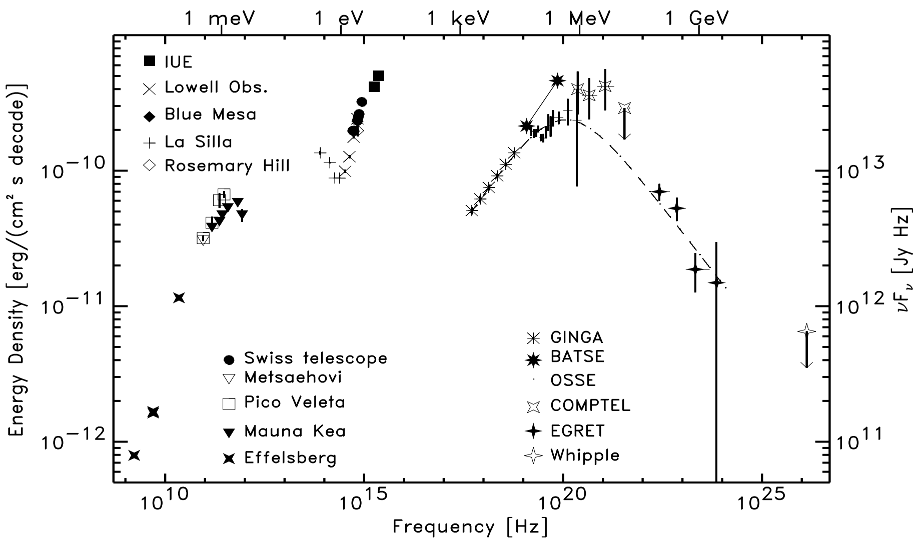


Fig. 8: Quasi-simultaneous broad-band spectrum of the blazar 3C 273 (Lichti et al. 1995).

electrons in the radio- and far-IR band, thermal emission from a dust torus in the IR and from an accretion disk in the UV ('blue bump'), and inverse Compton radiation generated by relativistic electrons and soft photons at X- and gamma-rays.

Figure 9 (Collmar et al. 1997) shows a non-simultaneous multifrequency spectrum of the blazar PKS 0528+134, which with a redshift of z=2.06 (Hunter et al. 1993) is a very far one. This spectrum shows probably only two maxima. One in the radio/infrared region and one in the $\gamma$-ray band, which clearly dominates the overall power output. The spectrum is interpreted to be completely of non-thermal origin with only two visible emission mechanisms at work: synchrotron emission from radio to optical and inverse Compton emission from X-rays to $\gamma$-rays(e.g. Böttcher and Collmar 1998). The source is too far away to show the thermal signatures from the dust torus and the accretion disk.

Figure 10 (from Dermer and Gehrels 1995) compares the high-energy luminosity spectra (assuming isotropic emission) of different sources and source classes as function of their rest frame energy. This figure allows to compare the amounts of radiated energy. The different spectral behaviour of blazars and Seyferts becomes clearly obvious from this diagram. It is obvious that the flat spectrum radio quasars (3C 279 as a bright example is shown) are by far the most luminous sources at these energies. The BL Lac objects (e.g. Mkn 421) can also be $\gamma$-ray emitters, but are usually less luminous than the quasars. However, in contrast to the quasars three BL Lac objects have been detected at TeV $\gamma$-

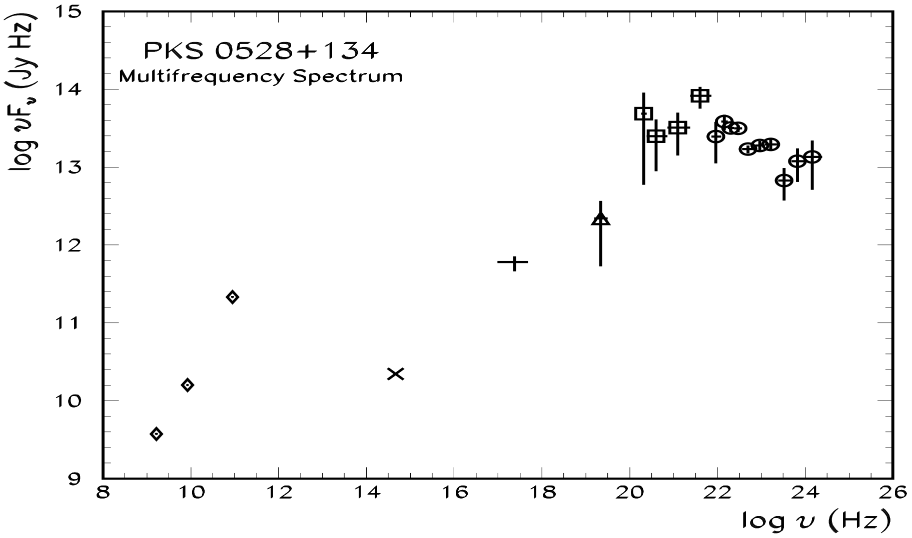


Fig. 9: Broad-band spectrum of PKS 0528+134 during a $\gamma$-ray high state (Collmar et al. 1997).

rays (Weekes et al. 1997). Only the closest Seyfert galaxies are observable at all (z<0.06). They are no $\gamma$-ray emitters because thermal spectra are observed which are assumed to originate from a hot thermal plasma (kT$\sim$30 keV) and cutoff at energies around $\sim$100 to $\sim$200 keV (e.g. NGC 4151 and IC 2943A).

Correlated monitoring observations have shown that detectable $\gamma$-ray emission in blazars is generally present in coincidence with enhanced radio activity. Sometimes correlated activity between $\gamma$-rays and other wavelength bands (e.g. X-rays, optical) has been observed. However, since the emission of these sources is always variable, these activities can not be correlated unambigously.

## 5 Model-independent Conclusions from Observations

Several observational facts for AGN in general and $\gamma$-ray blazars in particular have been summarized in the previous sections. In this section we want to apply some basic physical concepts to derive conclusions on physical parameters of active galaxies like their source of energy and their central masses.

The compactness of the central source is defined by the L/R-ratio, with L being its luminosity and R its radius. For a normal galaxy like our 'Milky Way' for example we derive an order of magnitude value of

$$\frac{L}{R} = \frac{10^{44}\,erg/s}{15\,kpc} = 2 \cdot 10^{21}\frac{erg/s}{cm} \tag{7}$$

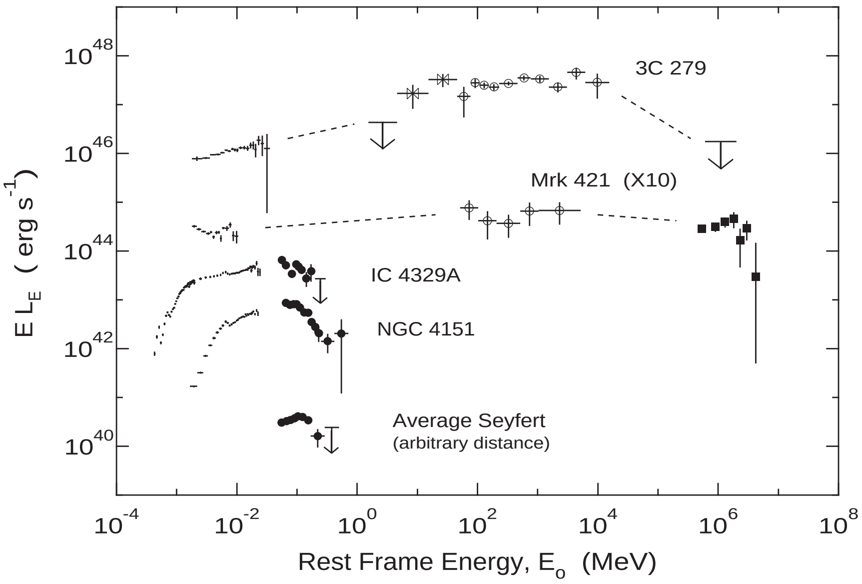


Fig. 10: Multiwavelength power spectra for the 'average' Seyfert galaxy, the bright Seyferts NGC 4151 and IC 4329A, the BL Lac-object Markarian 421, and the blazar 3C 279. The figure clearly shows, that in contrast to both blazars, the high-energy Seyfert spectra cut off around 100 keV, indicating thermal instead of a non-thermal spectra. The figure is from Dermer and Gehrels (1995).

However, for $\gamma$-ray blazars with luminosities of more than $\sim 10^{49}$ erg/s and time variability of less than a day, a compactness value of

$$\frac{L}{R} = \frac{10^{49}\, erg/s}{10^{15}\, cm} = 10^{34} \frac{erg/s}{cm} \tag{8}$$

is derived. The difference in compactness of more than 10 orders of magnitude clearly indicates the different source natures.

The luminosity of a normal galaxy is roughly the sum of the luminosity of its individual stars, and so is generated by nuclear fusion. In active galaxies is considerably more energy generated in much smaller volumes, even in a time-variable fashion. Only gravitation can provide more energy than nuclear fusion. If one assumes that a galaxy is a sphere of radius R, then for a given mass M the energy release from fusion and gravitation is equal, if

$$\frac{3}{5} \frac{GM^2}{R} = 0.007 M c^2, \tag{9}$$

with G the gravitational constant. Therefore the radius $R_{crit}$, for equal energy release is

$$R_{crit} = 43 \cdot \frac{2GM}{c^2} = 43 \cdot R_S. \tag{10}$$

If $R_{crit}$ is less than 43 Schwarzschild radii ($R_S$), energy generation by gravitation is more efficient than by nuclear fusion. Let us assume that an active galaxy would be powered by fusion then its maximal compactness is

$$\frac{L}{R} = \frac{E}{R_{crit} \cdot T_{life}} = \frac{0.007Mc^2}{43 \cdot \frac{2GM}{c^2} \cdot T_{life}} = 5 \cdot 10^{29} \frac{erg/s}{cm} \tag{11}$$

for a lifetime ($T_{life}$) of $10^8$ years. This result shows that fusion can at most provide a compactness of $10^{30}\frac{erg/s}{cm}$, which is in conflict to observations of AGN. Even this value is only an upper limit because nuclear fusion provides thermal energy which would have to be converted into non-thermal radiation energy as observed in blazars. In addition, the observed short-term variability in blazars is hard to understand if fusion is powering active galaxies. These arguments lead to the conclusion that active galaxies are powered by gravitational energy of a central massive object.

The AGN luminosity is generated by the release of gravitational energy of the infalling matter in the gravitational field of a central massive object. The mass of this object can be estimated by the physics of the accretion process. The so-called Eddington limit describes the balance between the gravitational force and the radiation pressure on the accreting material. If the radiation pressure dominates the accretion stops. For spherical accretion in the Thomson regime the Eddington limit for the luminosity of a source as function of the central mass is given by

$$L_{Edd} = 1.3 \cdot 10^{38} \frac{M}{M_{\odot}} \frac{erg}{s}. \tag{12}$$

If a source is radiating at its Eddington limit with a luminosity of $10^{46}$ erg/s, its mass is of the order of $10^8\,M_{\odot}$. Therefore nuclei of active galaxies should have masses in the range between $10^6\,M_{\odot}$ and $10^{10}\,M_{\odot}$. If the source is radiating below the Eddington limit, even larger masses would result.

The Eddington limit of the accretion process provides also clues on the build-up times and the lifetimes of AGN. The released gravitational energy has to be converted into the observed radiation energy:

$$L = \epsilon \cdot \dot{m}_{acc} c^2, \tag{13}$$

with L being the source luminosity, $\epsilon$ the efficiency for converting gravitational energy into radiation, $\dot{m}_{acc}$ the mass accretion rate, and c the speed of light. This equation has two consequences. Firstly, massive central objects of $10^8\,M_{\odot}$ can not be build up quickly, because at high accretion rates the corresponding strong outpushing radiation stops the accretion process. Secondly, the 'active' lifetimes of AGN are limited. After the source has accreted all material from its surroundings the activity stops. An $\epsilon$ of 0.1, which is the favoured number to date, leads to build-up timescales of the order of $10^8$ to $10^9$ years and lifetimes of the order of several times $10^8$ years for typical accretion rates of $\sim$1 to $\sim$2 $M_\odot$ per year. The powering of AGN by gravitational energy implies that bright active galaxies could not exist very early in the universe (unless they are born very massive) and can not shine forever. Their brightness ultimately has to stop, when they simply have 'eaten up' their host galaxies. Because they are not radiating forever, many 'normal' galaxies might contain 'quiet' massive centers, which are not 'fed' anymore.

Blazars emit polarized non-thermal radio emission: synchrotron radiation. This fact proves the presence of magnetic fields and relativistic electrons as well as an operating acceleration mechanism for the electrons. For large compactness, $\frac{L}{R} \geq 10^{30} \frac{erg/s}{cm}$, the relativistic electrons can not escape without interacting with their own synchrotron photons by the inverse Compton process, i.e. boosting the self-generated synchrotron photons to higher energies like X- and $\gamma$-ray energies. So high-energy emission is a natural consequence of high compactness and the presence of relativistic electrons.

The large $\gamma$-ray luminosities of blazars together with the observed short-term variability implys a highly compact emission region of the $\gamma$-ray radiation as well. For photons above the threshold energy $m_e c^2 = 511$ keV, the optical depth for pair production of a source of size R is given by $\tau_{\gamma\gamma} = n_\gamma \sigma_p R$, with $n_\gamma$ the photon density and $\sigma_p$ the cross section for pair production. A source will be optically thick for pair production if (e.g. Peterson 1997)

$$\tau_{\gamma\gamma} = \left(\frac{L_\gamma}{4\pi R^2 m_e c^3}\right) \sigma_e R = \frac{\sigma_e}{4\pi m_e c^3} \cdot \frac{L_\gamma}{R} = 2 \cdot 10^{-30} \frac{cm\, s}{erg} \cdot \frac{L_\gamma}{R} \geq 1, \qquad (14)$$

where $\sigma_e$ is the Thomson cross section, $L_\gamma$ the $\gamma$-ray luminosity, and R the source radius. For isotropic luminosities of $10^{48}$ erg/s and radii of $2.6 \cdot 10^{15}$ cm (1 light day), as observed in the $\gamma$-ray blazar 3C 279 for example, an optical depth for pair production of

$$\tau_{\gamma\gamma} = 770 \qquad (15)$$

is derived, which simply means that $\gamma$-rays can not ecape from such a source region without generating electron/positron pairs. Nevertheless, these $\gamma$-rays are observed! So, they have to come from an optically thin region. To resolve this contradiction, beamed emission from a relativistic jet is considered instead of central isotropic emission which was assumed in the calculations above. A jet origin of the observed $\gamma$-rays is consistent with the facts that for many blazars superluminal motion has been observed which is indicative for jets with a small offset angle from our line-of-sight, and with the redshift distribution of these sources, which shows that the source distance is not the critical parameter for their detection because $\gamma$-ray blazars are observed far out into the universe up to redshifts of z=2.3 (Hartman et al. 1997). A relativistic jet origin of the $\gamma$-rays would imply beamed emission. For beamed emission the angle between the photons is nearby zero therefore absorption by pair production is shifted to extremely high $\gamma$-ray energies (see equ. 5). The beamed emission has another effect:

the observed $\gamma$-ray luminosity overestimates the internal generated luminosity by a factor of up to $\sim 10^4$ due to relativistic Doppler boosting of the emitted photons and the solid angle effect. Therefore internally the optical depth for pair production is well below 1, which is in accord with the observation of these $\gamma$-rays. A luminosity reduction of up to $10^4$ does not change the conclusion reached above on the issue whether nuclear fusion or graviational energy powers active galaxies, because 1) the given upper limit for compactness does not contain an efficiency factor for conversion of thermal energy to non-thermal energy and 2) the observed short-term variability in blazars is not conceivable to be powered by fusion.

# 6 Models for the Gamma-ray Emission of Blazars

Since the CGRO discovery of $\gamma$-ray blazars, the origin of their $\gamma$-ray emission has been widely discussed. The models have been developed within the framework of the standard picture of radio-loud AGN (Fig. 3). Isotropical core emission has to be excluded. The compactness of the emission region inferred from the observed $\gamma$-ray fluxes and time variability would lead to severe absorption of the $\gamma$-ray radiation by pair production. The favoured scenario to explain the blazar radio-through-optical continua is that we are viewing nearly along the axis of a relativistically outflowing plasma jet which has been ejected from an accreting supermassive black hole. This broadband radiation is thought to be produced by non-thermal electron synchrotron radiation in outflowing plasma blobs. Figure 11 sketches the central part of an AGN, where according to models the $\gamma$-ray emission is generated. The high-energy blazar continuum emission appears to constitute a distinct second component in the broadband spectral energy distribution of blazars. Two classes of models have been proposed to explain the blazar $\gamma$-radiation, where either leptons or hadrons are the primary accelerated particles, which then radiate directly or through the production of secondary particles which in turn emit photons.

## 6.1 Leptonic Models

In leptonic models, the $\gamma$-ray emission of blazars is produced by non-thermal relativistic leptons (electrons and positrons) which scatter soft photons to $\gamma$-ray energies via the inverse-Compton (IC) process. These leptonic models come in two flavors depending on the nature of the soft photons. The synchrotron-self Compton models (SSC) assume the SSC process to be dominant. In this process (e.g. Maraschi et al. 1992, Bloom and Marscher 1993) the relativistic electrons moving along the magnetized jet generate synchrotron photons which are boosted by the same relativistic electron population to $\gamma$-ray energies via the IC-process. The IC-spectrum follows to first order the shape of the synchrotron spectrum (just shifted to higher energies), which explains the observed spectral turnover at MeV-energies in the $\gamma$-ray spectra.

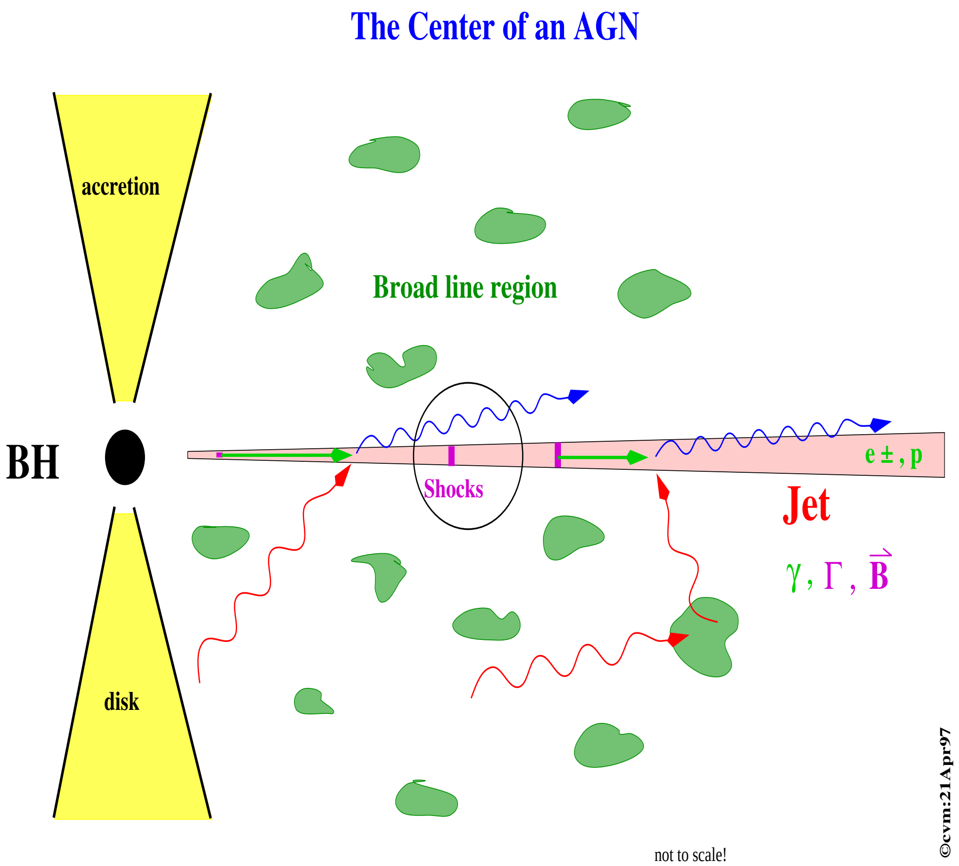


Fig. 11: Sketch (not scaled) of the inner part of an active galaxy. The $\gamma$-ray emission is thought to be generated in the inner jet region, a few hundreds of Schwarzschild radii apart from the central supermassive BH, where blobs of relativistic particles are injected and accelerated in the jet. The figure is from v. Montigny (1997).

The so-called external Compton scattering (ECS) models consider a different origin for the soft photons. They assume the soft X-ray and UV-photons which are radiated from the accretion disk directly into the jet (e.g. Dermer and Schlickeiser 1993) or scattered into the jet by the broad line region clouds (Sikora et al. 1994), to be the soft target photons for the relativistic jet electrons. The ECS-models also can reproduce the broad-band non-thermal spectral shape of the $\gamma$-ray blazars. These models explain the spectral bending at MeV-energies by the so called incomplete Compton cooling of the electrons. When a blob of relativistic electrons is injected into the jet, a power-law shaped IC-spectrum is generated with low - and high-energy cutoffs corresponding to the low - and high-energy cutoffs in the electron spectrum. Because the high-energy photons cool first, the high-energy cutoff in the IC-spectrum moves towards lower energies with time. The electron cooling by the IC-process stops when the blob has moved out into regions where the photon field becomes too thin to maintain this process. Integrating these spectra over time and over many outmoving blobs generates the spectral turnover at MeV energies observed by CGRO in time-averaged (days to weeks) $\gamma$-ray spectra (Dermer and Schlickeiser 1993).

### 6.2 Hadronic Models

Models have also been proposed in which accelerated hadronic particles (mainly protons) carry the bulk of the energy (e.g. Mannheim and Biermann 1992). Because protons do not suffer severe radiation losses, they can be accelereated up to energies of $10^{20}$ eV (Mannheim 1993), reaching the thresholds for photo-pion production, and the threshold for pion production in inelastic proton-matter collisions (Bednarek 1993). In these processes the protons transfer energy into photons, pairs, and neutrinos via pion production. The photons and pairs are reprocessed and initiate a cascade through inverse Compton and synchrotron processes to form a power-law photon spectrum in the end. Electrons and positrons generated via charged pion decay will be accompanied by energetic neutrino production. The detection of a strong neutrino flux from blazar jets would definitively identify hadrons as the primary radiating particles.

## 7 Summary and Conclusions

Recent $\gamma$-ray observations of AGN by CGRO have revealed a wealth of new informations on the $\gamma$-ray properties of AGN. Unexpectedly, blazar-type AGN have been found to be occasionally strong emitters of $\gamma$-ray radiation. On the other hand Seyfert-type AGN have not fulfilled the expectations. They are found to be strong emitters of hard X-ray radiation but no $\gamma$-ray emitting sources. These results fit well into the standard model of AGN and therefore provide strong support for this model, which assumes a supermassive BH as the central engine of active galaxies. The $\gamma$-ray blazars are sources in which a realativistic jet is more or less directly pointed towards us. The $\gamma$-ray luminosity produced in the jet is relativistically boosted and therefore becomes visible for the CGRO $\gamma$-ray telescopes.

Taking relativistic beaming into account, the internally generated $\gamma$-ray luminosities are estimated to be of the order of $10^{44}$ to $10^{45}$ erg/s (roughly the overall luminosity of our whole Milky Way), which is switched on and off on timescales of days. Only the release of gravitational energy in the field of a massive central object, which is the most efficient process known in nature, can provide the necessary energetics.

With isotropic luminosities up to $10^{44}$ erg/s (Dermer and Gehrels 1995) mass estimates via the Eddington limit provide central masses of the order $10^6$ to $10^7\,M_\odot$ for Seyferts. For blazars $10^8$ to $10^{10}\,M_\odot$ have been estimated from $\gamma$-ray observations (e.g. McNaron-Brown et al. 1995, Collmar et al. 1997). However, since the emission in blazars is probably beamed, the derived blazar masses have to be taken with caution.

According to models explaining the $\gamma$-ray emission of blazars, the $\gamma$-ray observations probe the physics of the inner jet region. They assume the injection of $\gamma$-ray radiating blobs at distances of several hundreds Schwarzschild radii ($100 < R_S < 300$) from the central engine. For a central mass of $10^8 M_\odot$ 500 $R_S$ are $\sim 1.5 \cdot 10^{11}$km, $\sim$1000 AU or $\sim$25 times the size of the solar system. If these models are correct, only a BH is viable to be the central massive object. No other object like a massive star cluster, for example, is comprehensible of being stable in such a 'massive' environment.

The $\gamma$-ray blazars are found to be jet sources. The large energies involved in the $\gamma$-ray emission ultimately provided by the even larger kinetic energy of the AGN jet, which in turn is in the end supplied by the central engine, is - according to our current understanding of physics - only conceiveable to be due to gravitational energy release in the vicinity of a massive BH.

In the line of these arguments, the recent CGRO $\gamma$-ray observations of AGN provide clear evidence for massive BH in the nuclei of active galaxies.

## References


Antonucci, R.R.J., Miller, J.S. (1995): ApJ **297**, 621

Ballmoos, P., Diehl, R., Schönfelder, V. (1987): ApJ **312**, 134

Bednarek, W. (1993): ApJ **402**, L29

Bloom, S.D., Marscher, A.P. (1993): *AIP Conference Proceedings 280*, (St. Louis), 578

Böttcher, M., Collmar, W. (1998): A&A, submitted

Collmar, W. (1996): *Workshop on Gamma-Ray Emitting*, eds. J.G. Kirk, M. Camenzind, C. v. Montigny, S. Wagner (Heidelberg), 9

Collmar, W., Bennett, K., Bloemen,?, et al. (1997): A&A, in press

Dermer, C.D., Schlickeiser, R., (1993): ApJ **416**, 458

Dermer, C.D., Gehrels, N. (1995): ApJ **447**, 103

Hartman, R.C., Webb, J.R., Marscher, A.P. et al. (1996): ApJ **461**, 698

Hartman, R.C., Collmar, W., v. Montigny, C., Dermer, C.D. (1995): in *Proc. of the 4th Compton Symposium*, eds. J. Kurfess, C. Dermer, in press

Hunter, S.D., Bertsch, D.L., Hartman, R.C., et al. (1993): ApJ **409**, 134

Johnson, W.N., Zdziarski, A.A., Madejski, G.M.., et al. (1997): in *Proc. of the 4th Compton Symposium*, eds. J. Kurfess, C. Dermer, in press

Kanbach, G. (1996): *Workshop on Gamma-Ray Emitting*, eds. J.G. Kirk, M. Camenzind, C. v. Montigny, S. Wagner (Heidelberg), 1

Kellermann, K.I., Sramek, R., Schmidt, M., et al. (1989): AJ **98**, 1195

Lichti, G.G., Balonek, T., Courvoisier, T.J.-L., et al. (1995): A&A **298**, 711

Mannheim, K., Biermann, P.L. (1992): A&A **253**, L21

Mannheim, K. (1992): A&A **269**, 67

Maraschi, L., Ghisellini, G., Celotti, A. (1992): ApJ **397**, L5
McNaron-Brown, K., Johnson, W.N., Jung, G.V., et al. (1995): ApJ **451**, 692
v. Montigny, C. (1997): Talk at the '4th Compton Symposium', Williamsburg, 1997
Nolan, P., Bertsch, D.L., Chiang, J., et al. (1996): ApJ **159**, 100
Perotti, F., Della Ventura, A., Villa, G., et al. (1981a): ApJ **247**, L63
Peterson, B. M. (1997): *An Introduction to active galactic nuclei* (University Press, Cambridge)
Robson, I. (1997): *Active Galactic Nuclei* (Wiley, Chichester, New York, Brisbane, Toronto, Singapure)
Perotti, F., Della Ventura, A., Villa, G., et al. (1981b): Nature **292**, 133
Schönfelder, V. (1995): *Physik in unserer Zeit* (Weinheim), 6/95, 262
Sikora, M., Begelman, M.C., Mitchel, C., et al. (1994): ApJ **421**, 153
Steinle, H., Bennett, K., Bloemen, H., et al. (1998): A&A, accepted
Swanenburg, B.N., Hermsen, W., Bennett, K., et al. (1978): Nature **275**, 298
Urry, M., Padovani, P. (1995): PASP**107**, 803
Weekes, T.C., Aharonian, F., Fegan, D.J., Kifune, T. (1997): in *Proc. of the 4th Compton Symposium*, eds. J. Kurfess, C. Dermer, in press